Phase space of electron- and muon-neutrino and antineutrino scattering off nuclei

M. Martini

IPSA-DRII, 63 boulevard de Brandebourg, 94200 Ivry-sur-Seine, France
and Sorbonne Université, CNRS/IN2P3, Laboratoire de Physique Nucléaire et de Hautes Energies (LPNHE), Paris, France

M. Ericson

Université Lyon, Université Claude Bernard Lyon 1, CNRS/IN2P3, IP2I Lyon, UMR 5822, F-69622, Villeurbanne, France
and Theory division, CERN, CH-12111 Geneva, Switzerland

G. Chanfray

Université Lyon, Université Claude Bernard Lyon 1, CNRS/IN2P3, IP2I Lyon, UMR 5822, F-69622, Villeurbanne, France

We discuss the electron and muon neutrino and antineutrino double-differential cross sections on carbon in the quasielastic as well as in the multinucleon and one pion production channels. By projecting them in the transferred momentum—transferred energy plane and in the neutrino energy—lepton scattering angle plane, as well as by performing simple considerations on the position of the quasielastic and Delta peaks and on their broadening, we explain the surprising dominance of the muon neutrino and antineutrino cross sections over the electron ones in particular kinematical conditions.

I. INTRODUCTION

One of the main objectives of present [1,2] and future [3–5] accelerator-based neutrino oscillation experiments is the search for the charge-parity (CP) violation in the leptonic sector. The best way to observe this phenomenon would be the measurement of a different appearance probability for electron neutrinos and electron antineutrinos from intense beams of muon neutrinos and muon antineutrinos. The next generation long-baseline (LBL) experiments will have unprecedented statistics of detected neutrinos thanks to intense beams and huge detector size. However these features are not sufficient to guarantee their success in the potential discovery of CP violation. In contrast with old bubble-chamber experiments, where the interaction of the neutrinos occurs with hydrogen, the use of relatively heavy nuclear targets (carbon, oxygen, argon), while allowing for a substantial increase of the event rate, requires a quantitative description of the nuclear response to weak interactions [6,7]. A precise and simultaneous knowledge of the ν_μ, ν_e, $\bar{\nu}_\mu$, and $\bar{\nu}_e$ cross sections on the target nucleus will be indeed crucial for the success of the LBL experiments.

In this connection, the last fifteen years have been characterized by numerous ν_μ and $\bar{\nu}_\mu$ cross sections measurements.

On the contrary the equivalent data for ν_e, and $\bar{\nu}_e$ are scarce and unlikely to reach the same level of precision as the ν_μ and $\bar{\nu}_\mu$ ones. A theoretical investigation on the difference between electron and muon cross sections is hence particularly important.

In charged current processes

$$\nu_l + A \rightarrow l^- + X, \tag{1}$$

$$\bar{\nu}_l + A \rightarrow l^+ + X, \tag{2}$$

where l denotes the generic flavor (which can be e or μ), ν_e ($\bar{\nu}_e$) cross sections are expected to be larger than the ν_μ ($\bar{\nu}_\mu$) ones due to the differences in the mass of the outgoing charged lepton, which imply different kinematic limits. This is certainly true for the total neutrino cross section σ_{ν_l} as a function of the neutrino energy E_{ν_l}. However this hierarchy can be opposite in specific kinematical conditions in the case of differential cross sections, as $d\sigma/[d\cos\theta]$, where θ is the lepton scattering angle, and $d^2\sigma/[dE_l d\cos\theta]$, where E_l is the charged-lepton energy, or equivalently $d^2\sigma/[d\omega d\cos\theta]$, where ω is the transferred energy, $\omega = E_{\nu_l} - E_l$.

This surprising inversion of the ν_e and ν_μ cross-section hierarchy was pointed out at first in Ref. [8] where it was shown that for forward-scattering angles the muon neutrino quasielastic differential cross sections can be larger than the corresponding electron ones, especially for low neutrino energies. This unexpected feature, and its potential important impact for the LBL neutrino oscillation results, pushed the community to perform further investigation in this direction. Hence several papers on this subject have been published [9–12]. Reference [8] already stressed that the surprising

dominance of ν_μ over ν_e quasielastic differential cross sections at fixed kinematics for small scattering angles is related to the differences in the momentum transfer $\mathbf{q} = \mathbf{k}_{\nu_l} - \mathbf{k}_l$ between the ν_e and ν_μ scattering. Reference [9] analyzed the (q, ω) phase space available for the charged current quasielastic (CCQE) interaction and pointed out that the ν_μ over ν_e dominance, appearing in the Fermi-Gas based and Hartree-Fock based approaches [8], could no more appear by considering a spectral function approach. However in the calculations of Ref. [9] nucleon final-state interactions were not taken into account. References [10,11] used several independent mean-field based models to conclude that a proper quantum-mechanical treatment of Pauli blocking and of the final nucleon's wave function confirms the dominance of ν_μ over ν_e cross sections at forward lepton scattering angle. In Ref. [12] the potential for mis-modeling of ν_e/ν_μ and $\bar{\nu}_e/\bar{\nu}_\mu$ CCQE cross-section ratios was quantified in order to investigate its impact on neutrino oscillation experiments. In this analysis large differences between the Hartree-Fock based and spectral function approaches appeared in the forward-scattered region and, even if less pronounced that in the Hartree-Fock case, a region where the $\nu_e/\nu_\mu < 1$ appeared also in the spectral function case for small neutrino energy. Furthermore, it was also shown that for the antineutrino case a region appears in the (θ, E_ν) phase space where $\bar{\nu}_e/\bar{\nu}_\mu < 1$. This happens at backward-scattering angles for different theoretical models.

In the present work we want to complement the previous investigations by performing phase-space and kinematical analysis which allows us to formulate simple and original explanations, not explicitly done in any of the previous published papers [8–12], of the surprising ν_μ over ν_e dominance in the quasielastic channel. The same analysis is generalized also to the other channels included in our approach [13], i.e., the multinucleon emission, the incoherent and coherent one pion production, marginally discussed only in Ref. [8] and omitted in Refs. [9–12] which focused on quasielastic only.

Although neutrino beams are not monochromatic, we decide to consider, as in all the previous theoretical papers on this subject [8–11], only the case of fixed neutrino energy. This variable E_{ν_l}, as well as the transferred energy ω and momentum q, is not directly measurable and up to now the neutrino scattering community rightly privileged the flux integrated cross sections as a function of measured variables such as the lepton energy E_l and the scattering angle θ. However there are several reasons to consider the cross sections also in terms of fixed neutrino energy. First we want to confine ourselves to the same conditions as those of the previous published analyses on the same subject [8–11]. Second, present and future neutrino detectors will allow more and more exclusive measurements and to know better and better the vertex activity. This, combined with more and more accurate neutrino interaction modeling, will allow to reconstruct and constrain unmeasured variables. First examples of experimental cross sections shown as a function of directly unmeasurable variables, such as $\sigma(E_{\nu_\mu})$, $d\sigma/d\omega$ [14] and, more recently, $[d^2\sigma(E_{\nu_\mu})]/[dk_\mu d\cos\theta]$ [15] already appeared. Finally it allows theoretical analyses and effective visualization of different cross sections behavior, as we show in the following.

II. QUASIELASTIC CHANNEL

Let us start by representing in the (q, ω) plane the charged current quasielastic double-differential cross sections $[d^2\sigma(E_{\nu_l})]/[d\omega d\cos\theta]$ on carbon for all the values of the scattering angle and for fixed values of the neutrino energy.

We remind that the values of $q = |\mathbf{q}|$ are obtained by the formula

$$q = \sqrt{E_{\nu_l}^2 + k_l^2 - 2E_{\nu_l}k_l\cos\theta}, \qquad (3)$$

where

$$k_l^2 = E_l^2 - m_l^2 = (E_{\nu_l} - \omega)^2 - m_l^2. \qquad (4)$$

Once E_{ν_l}, ω and $\cos\theta$ are fixed, q is determined, hence it is possible to project $d^2\sigma/[d\omega d\cos\theta]$ in the (q, ω) plane, the strength of the cross section being represented by a color chart. These cross sections, referring exclusively to the genuine CCQE channel, are shown in Figs. 1 and 2 for the four cases ν_e, ν_μ, $\bar{\nu}_e$, and $\bar{\nu}_\mu$, for the neutrino energies $E_{\nu_l} = 175$ MeV and $E_{\nu_l} = 575$ MeV, respectively. In the figures we show also the curves corresponding to the ω-q relation given by Eq. (3) for fixed values of the neutrino energy and charged-lepton mass for the two extreme values of the lepton scattering angle $\theta = 0$ and $\theta = \pi$. These curves delimit the available phase space.

Even if the figures are obtained by employing a peculiar approach, the random-phase approximation (RPA) one of Refs. [13,16,17], general considerations can however be made. First of all, some well-know features visually emerge:

(1) The electron (anti) neutrino phase space is larger than the corresponding muon one, due to the different charged-lepton mass, which explains the larger total cross sections in the electron case.

(2) The difference between the electron and muon (anti) neutrino cross sections decreases by increasing the neutrino energy.

(3) The antineutrino cross sections decrease more rapidly increasing q, hence increasing the angle, than the neutrino ones.

(4) The quasielastic response region clearly appears: all the cross sections are peaked at the quasielastic line[1]

$$\omega_{QE} = \frac{q^2 - \omega_{QE}^2}{2M_N} = \sqrt{q^2 + M_N^2} - M_N \qquad (5)$$

(M_N being the nucleon mass) and spread around this curve due to Fermi motion.

The most important feature which emerges from the figures, and which represents one of the original results of the present work, concerns the inversion of the ν_e ($\bar{\nu}_e$) and ν_μ ($\bar{\nu}_\mu$) cross-section hierarchy and it is the following:

(1) At lower neutrino energies (for example $E_{\nu_l} = 175$ MeV, as in Fig. 1) the $\theta = 0$ line largely crosses the quasielastic response region for the muon (anti)

_____

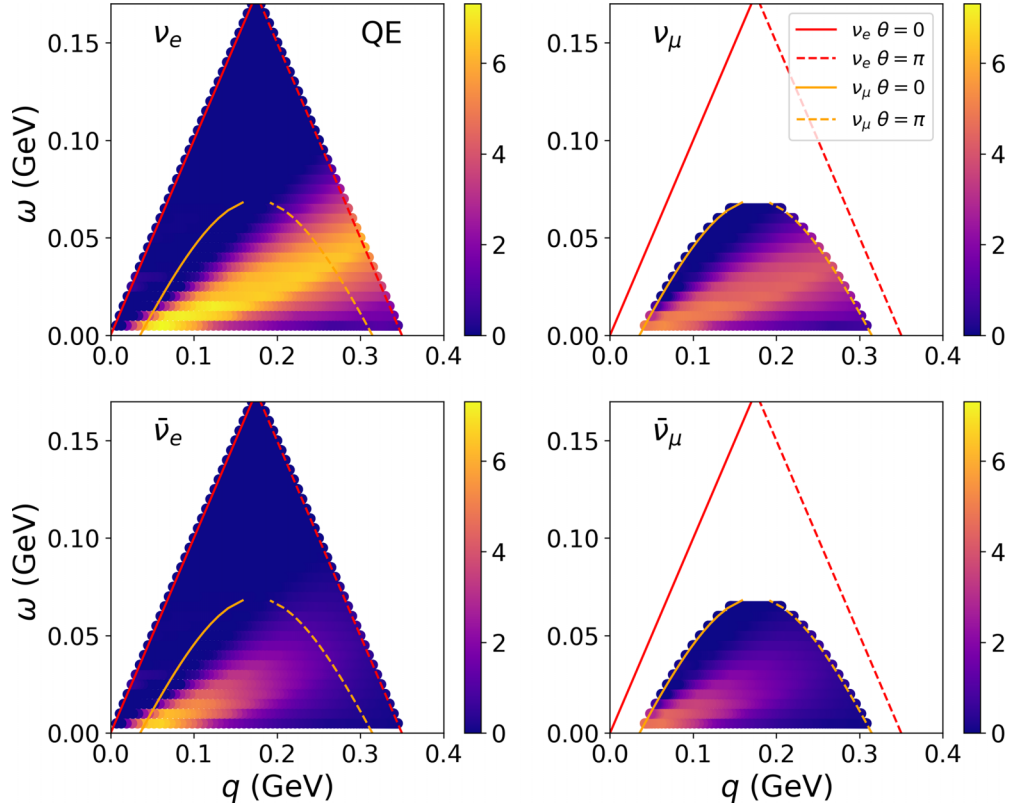[1] We remind that RPA collective effects may shift the position of the QE peak, but the effect remains relatively weak.

FIG. 1. Projection in the (q, ω) plane of the ν_e, ν_μ, $\bar{\nu}_e$, and $\bar{\nu}_\mu$ charged current quasielastic double-differential cross section on carbon $d^2\sigma(E_{\nu_l})/d\omega d\cos\theta$ for the fixed value of the neutrino energy $E_{\nu_l} = 175$ MeV and for all the values of the scattering angle. The strength of the cross section, in units of 10^{-38} cm^2/GeV, is given by the color scale. The curves corresponding to the ω-q relation given by Eq. (3) for fixed values of the neutrino energy and charged-lepton mass for the two extreme values of the lepton scattering angle, $\theta = 0$ and $\theta = \pi$, are also plotted.

neutrino scattering, which is not the case of electron (anti) neutrino scattering, where the $\theta = 0$ line is always outside the quasielastic response region. In other words, *for neutrino and antineutrino scattering the $\theta = 0$ muon and electron lines explore in the (q, ω) plane two different regions, the muon one corresponding to larger quasielastic cross sections*. By increasing the neutrino energies the difference between the muon and electron $\theta = 0$ lines decreases and the two curves explore more and more similar region in the (q, ω) plane, as it appears in Fig. 2.

The same argument allows us to see why at low neutrino energies the muon antineutrino cross sections are larger than electron ones also for backward-scattering angles, as first observed in Ref. [12]:

(1) At low neutrino energies for antineutrino scattering the $\theta = \pi$ muon and electron lines explore in the (q, ω) plane two different regions, the muon one corresponding to larger quasielastic cross sections, as appears in Fig. 1.

To deepen our analysis let us consider now the energy position of the quasielastic peak in terms of the lepton variables

E_{ν_l}, $\cos\theta$, and m_l,

$$\omega_{QE}^{m_l} \equiv \omega_{QE}\left(E_{\nu_l}, \cos\theta, m_l\right), \qquad (6)$$

obtained by solving Eq. (5) once q is expressed according to Eqs. (3) and (4). We omit to write its simple but long explicit expression, except in the case of zero charged-lepton mass, where it reduces to

$$\omega_{QE}^{m_l=0} = \frac{E_{\nu_l}^2(1 - \cos\theta)}{M_N + E_{\nu_l}(1 - \cos\theta)}. \qquad (7)$$

Depending on the values of E_{ν_l} and θ, one of the two possibilities is realized: $\omega_{QE}^{m_e} < \omega_{QE}^{m_\mu}$ or $\omega_{QE}^{m_\mu} < \omega_{QE}^{m_e}$. This is illustrated in Fig. 3 which shows the (θ, E_{ν_l}) and the $(E_{\nu_l}, \cos\theta)$ planes. In these planes the gray area delimits the region where $\omega_{QE}^{m_e} < \omega_{QE}^{m_\mu}$. One can observe that this situation occurs for small scattering angles and for very low values of $\omega_{QE}^{m_l}$, being $\omega_{QE}^{m_l} \lesssim 5$ MeV. For such very small values of ω_{QE}, the region where $\omega \geqslant \omega_{QE}$ would mainly contribute to the response. As a consequence, when $\omega_{QE}^{m_e} < \omega_{QE}^{m_\mu}$ (or, in other words when the ν_μ quasielastic peak is shifted at larger energies than the ν_e one) the contribution of the tail above the quasielastic peak will be larger for ν_μ than for ν_e, hence the ν_μ quasielastic cross section will be larger than the ν_e one. This is illustrated in Fig. 4 which shows the ν_e, ν_μ, $\bar{\nu}_e$, and $\bar{\nu}_\mu$ charged
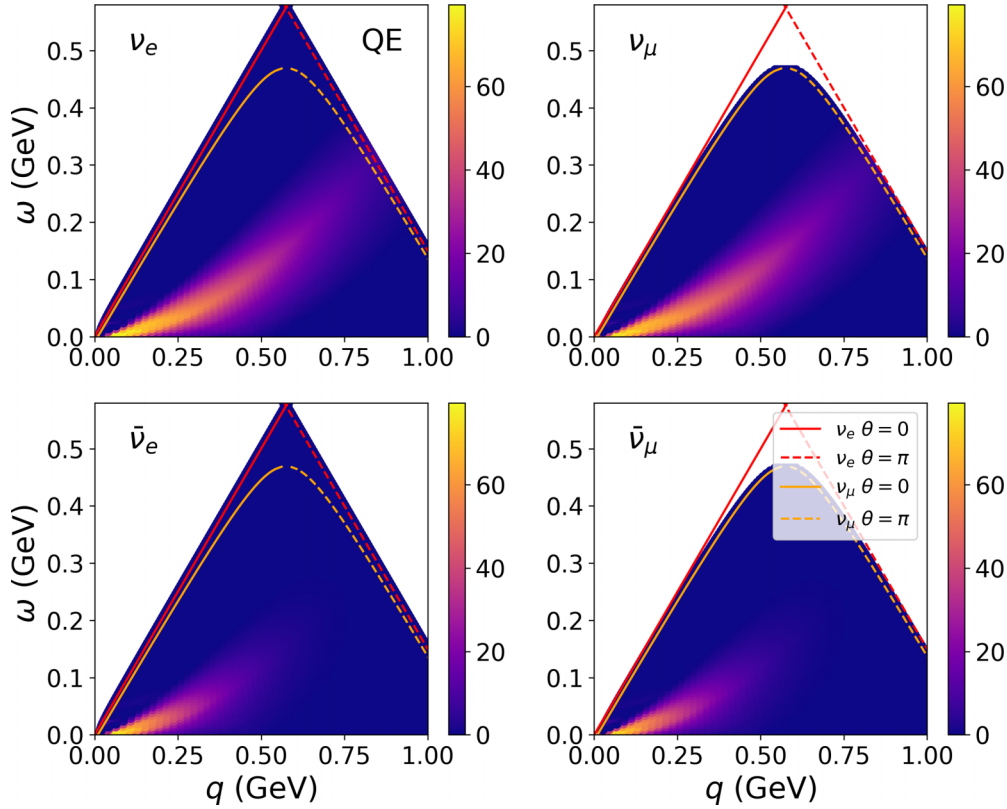
FIG. 2. The same as Fig. 1 but for $E_{\nu_l} = 575$ MeV.

current quasielastic double-differential cross sections on carbon $[d^2\sigma(E_{\nu_l})]/[d\omega d\cos\theta]$ for $E_{\nu_l} = 175$ MeV. The behavior described above appears for $\cos\theta = 0.98$, where $\omega_{QE}^{m_e} = 0.65$ MeV is lower than $\omega_{QE}^{m_\mu} = 1.24$ MeV.[2] On the other hand, for $\cos\theta = 0$, $\omega_{QE}^{m_e} = 27.49$ MeV is larger than $\omega_{QE}^{m_\mu} = 22.48$ MeV and the electron (anti) neutrino cross sections are larger than the corresponding muon ones.

—————

[2]The introduction of an additional parameter to take into account the nucleon binding energy would shift the position of ω_{QE} towards larger energies but would not alter our conclusion.

We have hence found the simple explanation on why the muon (anti) neutrino quasielastic cross sections can be larger than the electron ones: when $\omega_{QE}^{m_e} < \omega_{QE}^{m_\mu}$ the ν_μ quasielastic cross sections "falls after" the ν_e ones. This simple explanation is strongly supported by the close correspondence between the left panel of our Fig. 3 and the left panel of Fig. 4 of Ref. [10], both referring to the (θ, E_ν) plane: the region where $\omega_{QE}^{m_e} < \omega_{QE}^{m_\mu}$ (our Fig. 3) practically coincides with the region where the calculations of the cross sections lead to $\frac{d\sigma_e/d\cos\theta}{d\sigma_\mu/d\cos\theta} < 1$ (Fig. 4 of Ref. [10]).
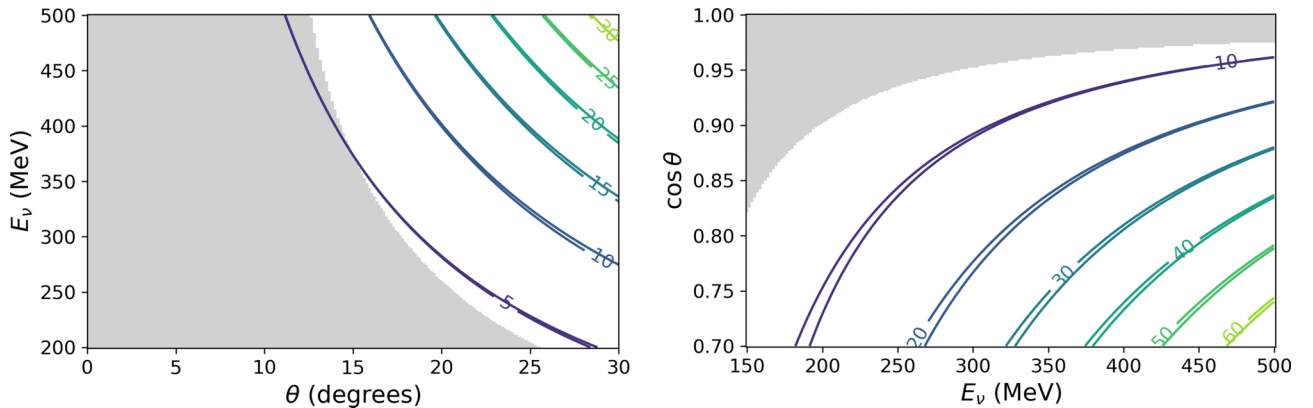

FIG. 3. Region, gray area, where $\omega_{QE}^{m_e} < \omega_{QE}^{m_\mu}$ in the (θ, E_{ν_l}) (left panel) and $(E_{\nu_l}, \cos\theta)$ (right panel) planes. Some constant values of $\omega_{QE}^{m_e}$ and $\omega_{QE}^{m_\mu}$ are represented by pair of continuous colored lines. The lines labeled by the ω_{QE} value (in MeV) are those corresponding to $\omega_{QE}^{m_e}$.
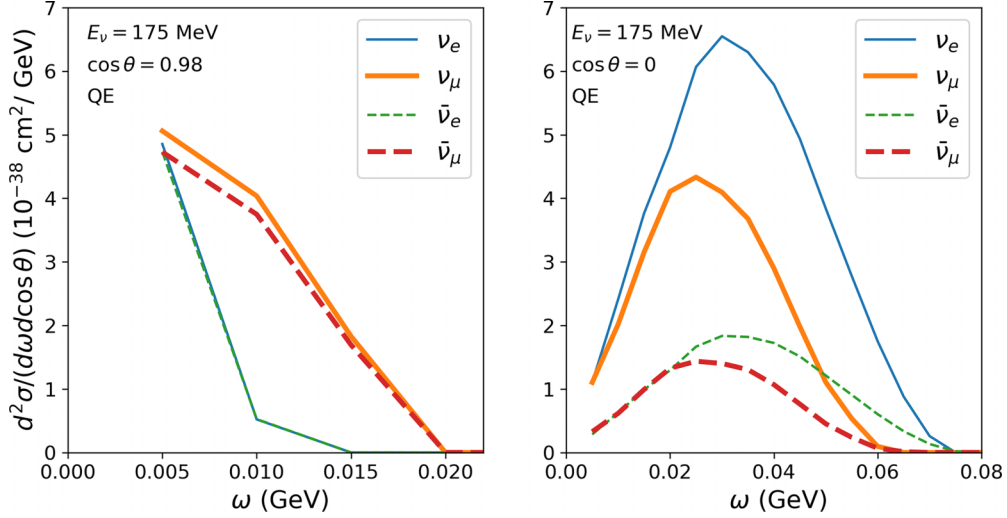
FIG. 4. The ν_e, ν_μ, $\bar{\nu}_e$, and $\bar{\nu}_\mu$ charged current quasielastic double-differential cross sections on carbon $\frac{d^2\sigma(E_{\nu_l})}{d\omega d\cos\theta}$ for the fixed value of the neutrino energy $E_{\nu_l} = 175$ MeV and for two different values of the scattering angle.

III. OTHER CHANNELS

Let us move now to the other channels described by our model, the multinucleon emission and the resonant and coherent one pion production, and let us start by showing, as for the quasielastic, the projection of the corresponding double-differential cross sections on the (q, ω) plane. The case of multinucleon emission, including 2p-2h and 3p-3h excitations, hence called np-nh, is shown in Fig. 5 for

$E_{\nu_l} = 175$ MeV and in Fig. 6 for $E_{\nu_l} = 575$ MeV. For this last value of the neutrino energy, the resonant one-pion production result is shown in Fig. 7 and the coherent pion one in Fig. 8.

From Figs. 5 and 6 one can observe that in the case of np-nh excitations the cross section, which reflects the nuclear response region, is not restricted to the Fermi motion band around the quasielastic line (as in Figs. 1 and 2) but it covers the major part of the (q, ω) plane. As a consequence the
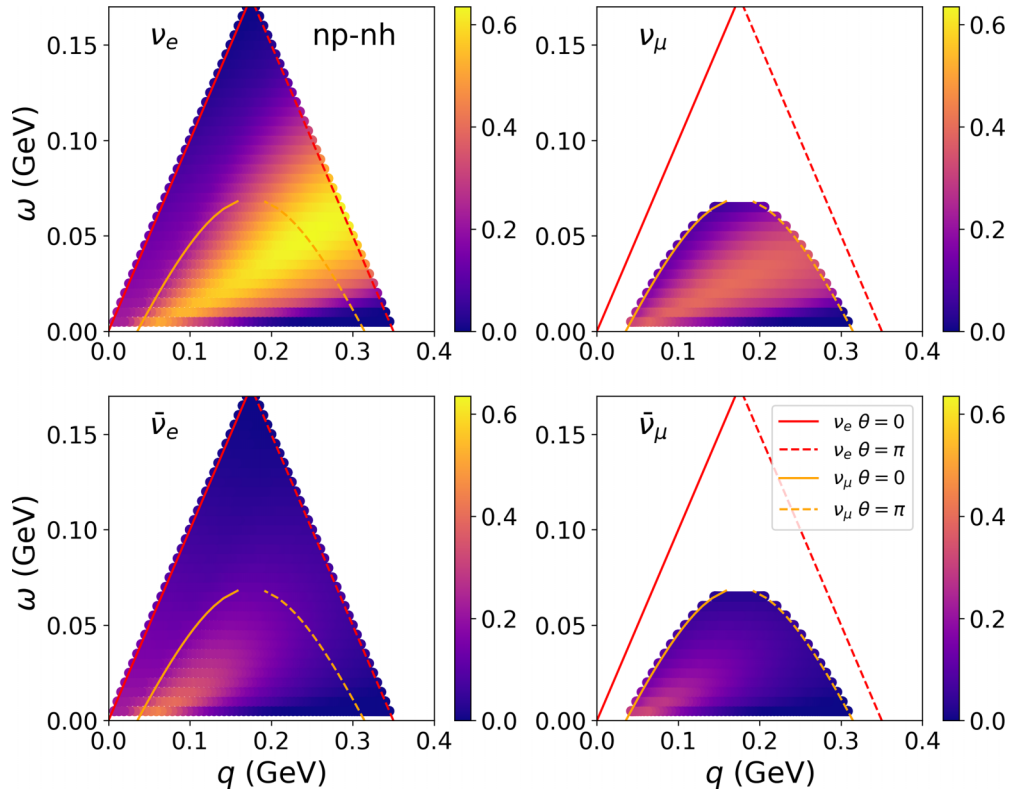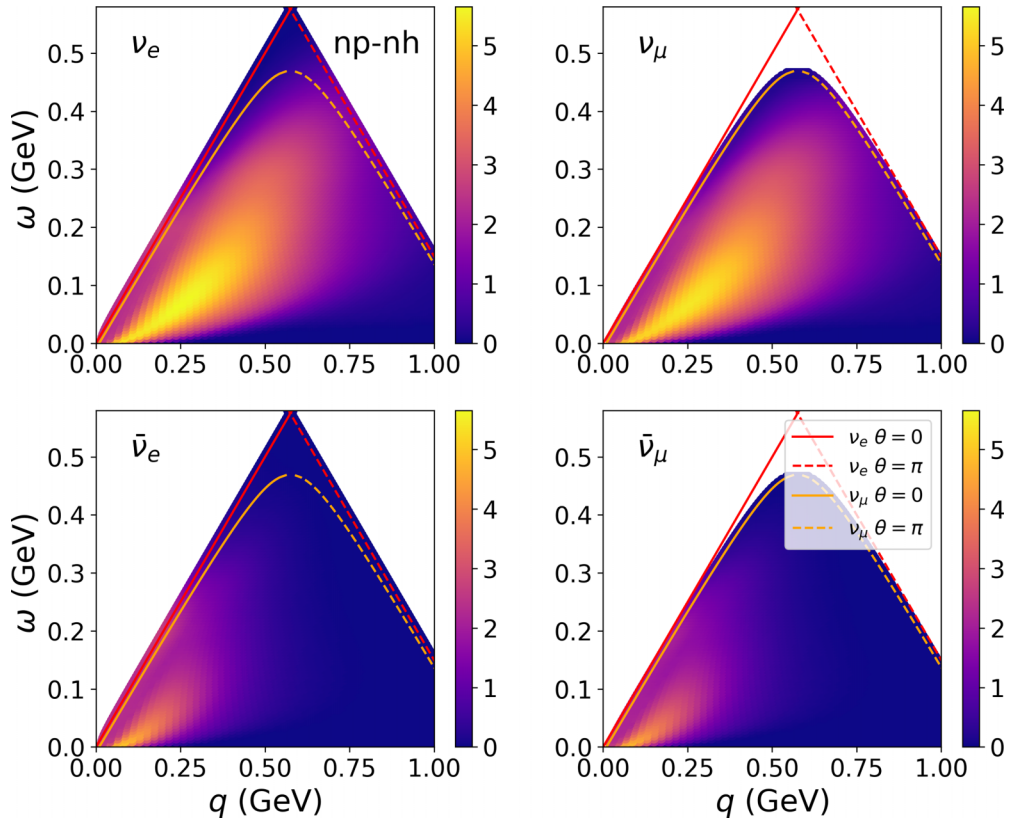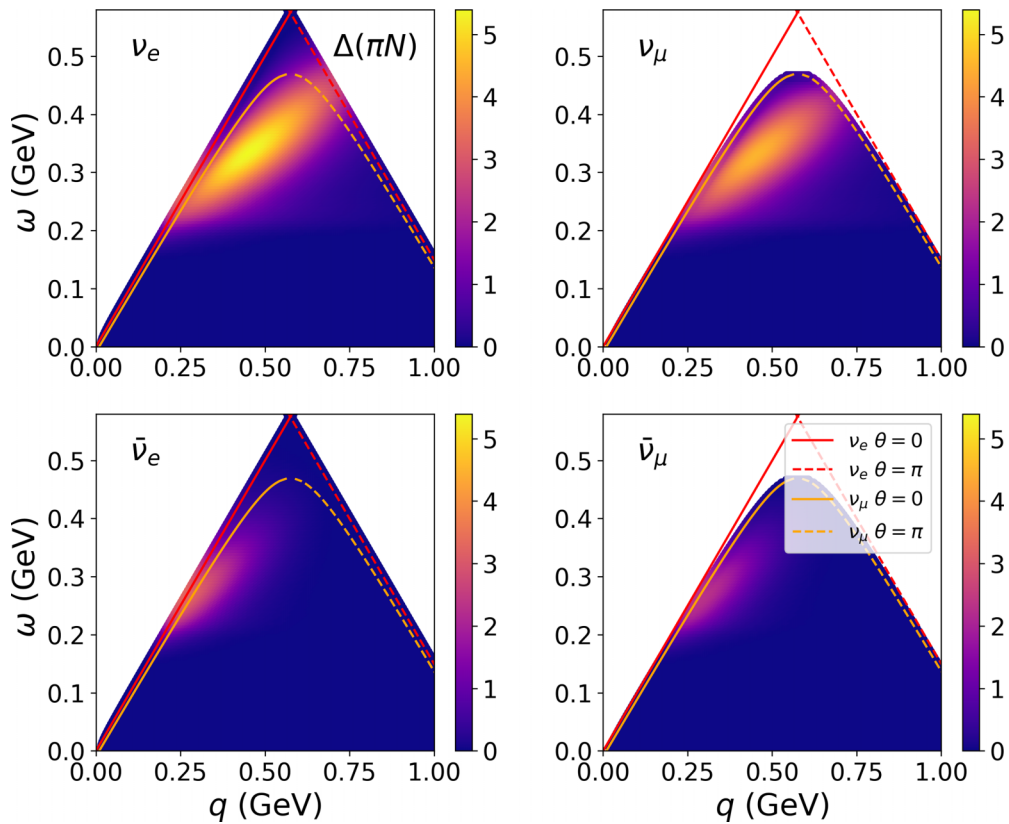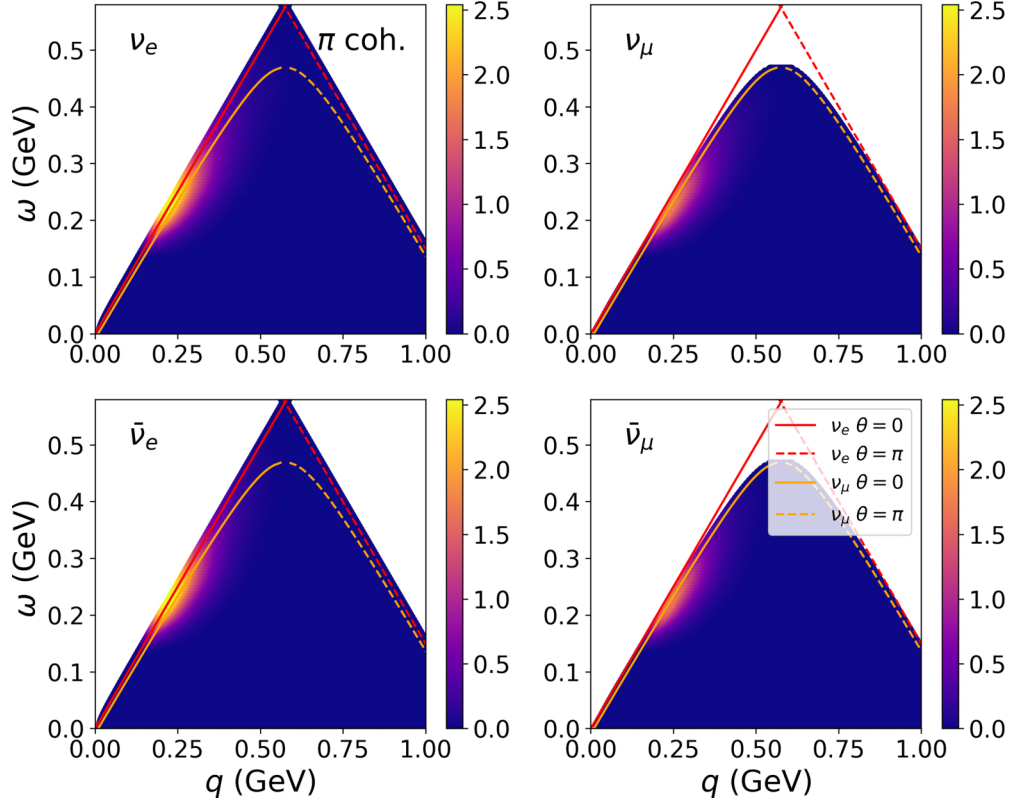

FIG. 5. The same as Fig. 1 at $E_{\nu_l} = 175$ MeV, but for np-nh excitations.

FIG. 6. The same as Fig. 1, but for np-nh excitations and $E_{\nu_l} = 575$ MeV.

FIG. 7. The same as Fig. 1, but for the one-pion production via Δ-resonance excitation and $E_{\nu_l} = 575$ MeV.

FIG. 8. The same as Fig. 1, but for the coherent one-pion production and $E_{\nu_l} = 575$ MeV.

intersection between the $\theta = 0$ line and the nuclear response, does not seem to clearly indicate the dominance of muon (anti) neutrino cross section over the electron ones at low neutrino energy, as for quasielastic. Some cases where this phenomenon locally survives are discussed later.

Concerning the incoherent one-pion production cross sections projected in the (q, ω) plane in Fig. 7, one can recognize the Δ-resonance response region peaked around the Δ-line

$$\omega_\Delta = \sqrt{q^2 + M_\Delta^2} - M_N. \tag{8}$$

By ignoring the charged-lepton mass, Eq. (8) can be written as

$$\omega_\Delta^{m_l=0} = \frac{M_N \Delta M + E_{\nu_l}{}^2 (1 - \cos\theta)}{M_N + E_{\nu_l}(1 - \cos\theta)}, \tag{9}$$

with $\Delta M = (M_\Delta^2 - M_N^2)/2M_N = 338$ MeV. Equation (9) is the corresponding of Eq. (7), related to quasielastic, in the case of Δ. The spread around the Δ line is due to the in-medium Δ width and to the Fermi motion.

Turning to the projection in the (q, ω) plane of the coherent 1 pion production cross sections, shown in Fig. 8, one can observe the accumulation of strength around the $\theta = 0$ line, which coincide with the $\omega = q$ line when $m_l = 0$, reflecting the free pion dispersion relation

$$\omega_\pi = \sqrt{q^2 + m_\pi^2}. \tag{10}$$

From Figs. 7 and 8 the resonant and coherent one-pion production (anti) neutrino double-differential cross sections seem

to be globally larger in the electron than in the muon case. It is however interesting to consider these cross sections for some fixed kinematics as a function of the transferred energy to investigate the possible emergence of some region where this hierarchy is opposite as well the appearance of other effects. For this purpose we plot in Fig. 9 this cross section at $E_{\nu_l} = 575$ MeV and $\cos\theta = 0.965$ for the resonant pion production channel. At this kinematics the position of the Δ peak is at larger ω for ν_μ than for ν_e, hence an effect analog to the one discussed above for quasielastic could in principle appears:
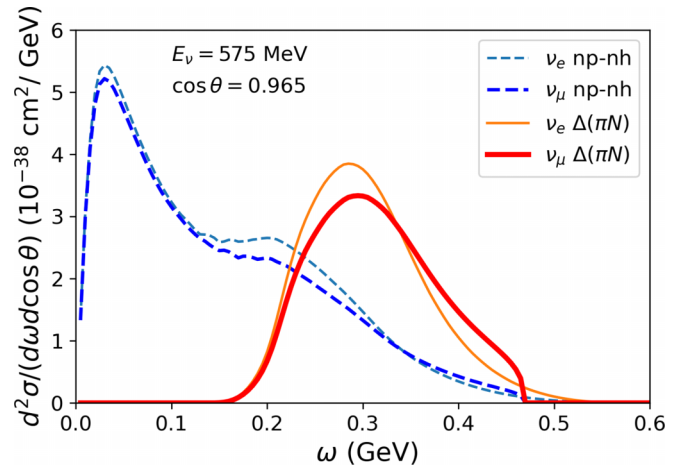
FIG. 9. The ν_e and ν_μ double-differential cross sections on carbon $\frac{d^2\sigma(E_{\nu_l})}{d\omega d\cos\theta}$ for np-nh excitations and for the resonant one-pion production at $E_{\nu_l} = 575$ MeV and $\cos\theta = 0.965$.
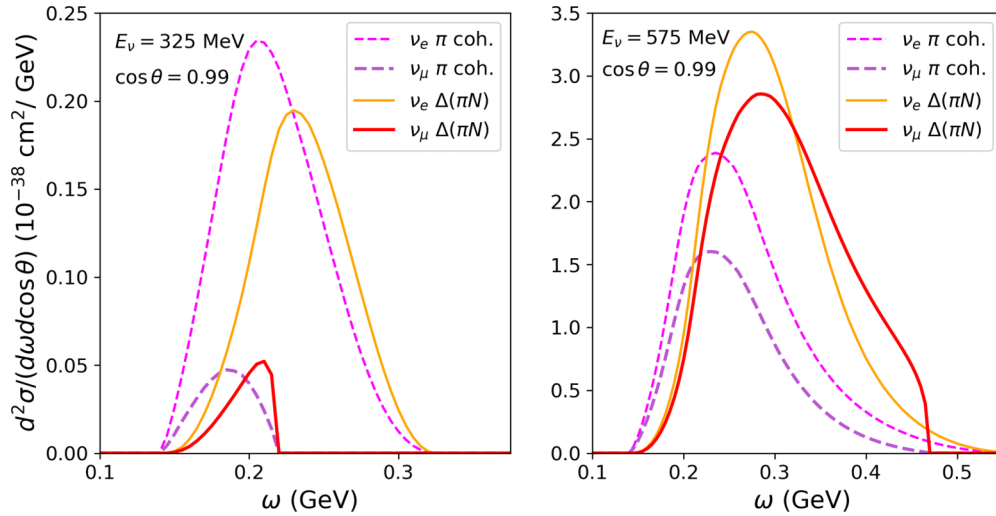
FIG. 10. The ν_e and ν_μ double-differential cross sections on carbon $\frac{d^2\sigma(E_{\nu_l})}{d\omega d\cos\theta}$ for coherent and resonant one-pion production at $E_{\nu_l} = 325$ MeV and $E_{\nu_l} = 575$ MeV and $\cos\theta = 0.99$.

the spread of the Δ width could shift the ν_μ cross section at larger ω leading to a larger cross section for ν_μ than for ν_e in the tail. Indeed this is what locally happens. However the effects is less evident than for the quasielastic. Furthermore, it is combined to threshold effects related to the finite muon mass, leading to peculiar shape of the ν_μ cross section near the maximum value of the allowed excitation energy. The same threshold effect as well as the dominance of the ν_μ over ν_e is also visible, even if weakly, in the tail of multinucleon cross section (plotted in Fig. 9 as well), the np-nh being due to the nonpionic decay of the Δ in this tail.

Figure 10 shows the coherent and resonant one-pion production double-differential cross sections at $\cos\theta = 0.99$ for two values of neutrino energy, $E_{\nu_l} = 325$ MeV and $E_{\nu_l} = 575$ MeV. Beyond to retrieve for the resonant cross section at $E_{\nu_l} = 575$ MeV the behavior already discussed for Fig. 9, one can observe that the coherent and the resonant cross sections are peaked at different energies, reflecting the differences between ω_π and ω_Δ. Furthermore at $E_{\nu_l} = 325$ MeV the maximum value of the cross section is larger for the coherent than for the resonant channel in the case of ν_e scattering.

IV. SUMMARY AND CONCLUSION

In summary we have explained why the ν_μ quasielastic differential cross sections can be larger than the corresponding ν_e

ones by analyzing the (q, ω) and the (θ, E_ν) phase spaces. We have found a simple criterium to determine when muon (anti) neutrino quasielastic differential cross sections are larger than the corresponding electron ones, based on the position of the quasielastic peak at very low transferred energy. This criterium, which does not need the explicit calculation of the cross sections, could be useful for experimental analyses allowing simple cuts to exclude regions where the modeling cross section is expected to be not so robust.

Also in the one pion production and in the multinucleon emission channels, for peculiar kinematical conditions, we have found in the tails of the double-differential cross sections as a function of the transferred energy a dominance of ν_μ over the ν_e results. The shape of these tails is also affected by threshold effects.

As a perspective, even if the correspondence between ν_e and ν_μ cross section is not trivial, one could use the representation of the cross sections in terms of the q and ω variables, as done in this work, to investigate if it is possible to find patterns allowing to constrain unmeasured electron (anti)neutrino cross sections starting from the measured muon ones.

[1] K. Abe *et al.* (T2K Collaboration), Nature **580**, 339 (2020); **583**, E16 (2020).

[2] M. A. Acero *et al.* (NOvA Collaboration), Phys. Rev. Lett. **123**, 151803 (2019).

[3] K. Abe *et al.* (Hyper-Kamiokande Proto-Collaboration), arXiv:1805.04163.

[4] R. Acciarri *et al.* (DUNE Collaboration), arXiv:1512.06148.

[5] A. Alekou *et al.*, Eur. Phys. J. Spec. Top. **231**, 3779 (2022).

[6] T. Katori and M. Martini, J. Phys. G **45**, 013001 (2018).

[7] L. Alvarez-Ruso *et al.* (NuSTEC Collaboration), Prog. Part. Nucl. Phys. **100**, 1 (2018).

[8] M. Martini, N. Jachowicz, M. Ericson, V. Pandey, T. Van Cuyck, and N. Van Dessel, Phys. Rev. C **94**, 015501 (2016).

[9] A. M. Ankowski, Phys. Rev. C **96**, 035501 (2017).

[10] A. Nikolakopoulos, N. Jachowicz, N. Van Dessel, K. Niewczas, R. González-Jiménez, J. M. Udías, and V. Pandey, Phys. Rev. Lett. **123**, 052501 (2019).

[11] R. González-Jiménez, A. Nikolakopoulos, N. Jachowicz, and J. M. Udías, Phys. Rev. C **100**, 045501 (2019).

[12] T. Dieminger, S. Dolan, D. Sgalaberna, A. Nikolakopoulos, T. Dealtry, S. Bolognesi, L. Pickering, and A. Rubbia, Phys. Rev. D **108**, L031301 (2023).

[13] M. Martini, M. Ericson, G. Chanfray, and J. Marteau, Phys. Rev. C **80**, 065501 (2009).

[14] P. Abratenko *et al.* (MicroBooNE Collaboration), Phys. Rev. Lett. **128**, 151801 (2022).

[15] P. Abratenko *et al.* (MicroBooNE Collaboration), arXiv:2307.06413.

[16] M. Martini, M. Ericson, and G. Chanfray, Phys. Rev. C **84**, 055502 (2011).

[17] M. Martini and M. Ericson, Phys. Rev. C **87**, 065501 (2013).